Elastic Interferometry by Multi-Dimensional Deconvolution in the presence of intrinsic losses and uncorrelated noise

Joost van der Neut[*]*, Kees Wapenaar, Jan Thorbecke and Evert Slob*
Delft University of Technology, Delft, the Netherlands

Summary

Our aim is to redatum multi-component sources from their actual location near the earth surface to multi-component receiver locations in a horizontal borehole, without requiring any information about the medium between sources and receivers. For this purpose we use elastic interferometry by Multi-Dimensional Deconvolution (MDD). We show how MDD is related to Cross-Correlation-based (CC) redatuming techniques such as the Virtual Source method. We test the accuracy of MDD on a 2D synthetic elastic model in the presence of intrinsic losses and background noise. We observe that loss terms are handled correctly and that MDD is numerically stable under the corruption of uncorrelated noise.

Introduction

Recently, various cross-correlation (CC) based techniques have emerged to redatum source locations to subsurface receivers without requiring a velocity model of the medium between sources and receivers. Examples include the Virtual Source method (Bakulin and Calvert, 2006), Interferometric Imaging (Schuster et al., 2004) and other forms of Seismic Interferometry (Wapenaar et al., 2008a). The underlying theory generally relies on a closed boundary of sources surrounding the receivers and the assumption of a lossless medium. In practice, these methods are often applied to cases with one-sided illumination and intrinsic losses may be significant. As a consequence, spurious events can emerge and seismic amplitudes of retrieved data will generally be incorrect (Snieder et al., 2006). Alternatively, we can apply Seismic Interferometry by Multi-Dimensional Deconvolution (MDD) (Wapenaar et al., 2008b). This method can be applied in general anisotropic inhomogeneous dissipative media and it has the ability to compensate for anisotropic illumination (Wapenaar et al., 2008c). We review the theory of MDD-based interferometry and show its relation to CC-based methods. Then we introduce a simple synthetic 2D elastic model to test the stability of MDD in the presence of intrinsic losses and uncorrelated noise.

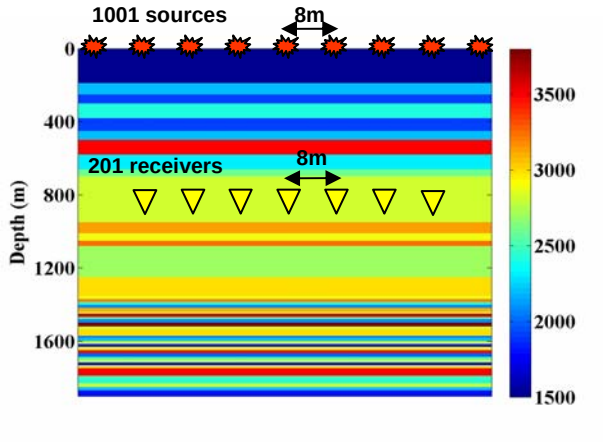

Figure 1: Configuration. 1001 multi-component sources are located near the earth surface with 8m spacing. 201 multi-component receivers are located at 800m depth with 8m spacing. Shown is the P-wave velocity model in m/s.

Theory

The configuration for a typical experiment of our interest is shown in Figure 1. We assume to have multi-component sources at the surface and registrations of particle velocity $\hat{\mathbf{v}}(\mathbf{x}_R,\mathbf{x}_S,\omega)$ and tractions $\hat{\boldsymbol{\tau}}(\mathbf{x}_R,\mathbf{x}_S,\omega)$ in a borehole at depth, where $\mathbf{x}_R$ is the receiver location, $\mathbf{x}_S$ the source location and ω the angular frequency (the circumflex denotes the space-frequency-domain). Each source-receiver pair is then decomposed into a flux-normalized downgoing field $\hat{\mathbf{p}}^{+}(\mathbf{x}_R,\mathbf{x}_S,\omega)$ and upgoing field $\hat{\mathbf{p}}^{-}(\mathbf{x}_R,\mathbf{x}_S,\omega)$ by the following operation:

$$\begin{pmatrix}\hat{\mathbf{p}}^{+}\\ \hat{\mathbf{p}}^{-}\end{pmatrix}=\hat{\mathscr{L}}^{-1}\begin{pmatrix}\hat{\mathbf{p}}\\ \hat{\mathbf{v}}\end{pmatrix}, \qquad (1)$$

where $\hat{\mathscr{L}}^{-1}$ is a decomposition operator; depending on the medium parameters at the receiver level; see Wapenaar et al. (2008b) for details. The decomposed wave fields can be represented as $\hat{\mathbf{p}}^{\pm}=\left(\hat{\Phi}^{\pm}\quad\hat{\Psi}^{\pm}\quad\mathrm{Y}^{\pm}\right)^{T}$, where $\hat{\Phi}^{\pm}$, $\hat{\Psi}^{\pm}$ and $\mathrm{Y}^{\pm}$ are representations of the down- or upgoing P-, Sv and Sh-wave potential, respectively. The decomposition is scaled such that all wave fields are power-flux normalized.

Due to this normalization, it can be shown that the following reciprocity relation of the convolution type is satisfied:

$$\int_{\partial D1} \hat{\mathbf{p}}_A^+ \hat{\mathbf{p}}_B^- - \hat{\mathbf{p}}_A^- \hat{\mathbf{p}}_B^+ d^2\mathbf{x} = \int_{\partial D2} \hat{\mathbf{p}}_A^+ \hat{\mathbf{p}}_B^- - \hat{\mathbf{p}}_A^- \hat{\mathbf{p}}_B^+ d^2\mathbf{x}, \tag{2}$$

where the integrals are over any arbitrary depth levels ∂D_1 and ∂D_2. Subscripts A and B represent two wavefields in state A and B, respectively. In state B we choose the actual parameters, with a source at location $\mathbf{x}_S$, yielding the observed decomposed data $\hat{\mathbf{p}}_B^{\pm} = \hat{\mathbf{p}}^{\pm}(\mathbf{x}, \mathbf{x}_S, \omega)$. For state A we choose a reference medium, where the medium above the receiver array has been replaced by a homogeneous halfspace. We choose a source at location $\mathbf{x}_A$ just above the actual receiver array. We refer to this state with subscript zero; thus: $\hat{\mathbf{p}}_A^{\pm} = \hat{\mathbf{p}}_0^{\pm}(\mathbf{x}, \mathbf{x}_A, \omega)$. Level ∂D_1 is chosen as the receiver level. Since this level is situated right below the source location $\mathbf{x}_A$ and all inhomogenities above ∂D_1 have been removed in the reference state, the downgoing field at ∂D_1 can be interpreted as a 2D delta-function convolved with the source wavelet: $\hat{\mathbf{p}}_0^+ = \hat{S}\delta(\mathbf{x}_H - \mathbf{x}_{H,A})$, where subscript H denotes that only the horizontal coordinates are taken into account. We choose ∂D_2 as the deepest level where scattering occurs, such that $\hat{\mathbf{p}}^-(\mathbf{x}, \mathbf{x}_S, \omega) = 0$ and $\hat{\mathbf{p}}_0^-(\mathbf{x}, \mathbf{x}_S, \omega) = 0$ for $\mathbf{x} \in \partial D_2$. In practice these conditions can be satisfied by assuming the level to be deep enough such that all amplitudes are below the noise level. Substituting these boundary conditions into representation 2 and we find

$$\hat{\mathbf{p}}^-(\mathbf{x}_R, \mathbf{x}_S, \omega) = \int_{\partial D1} \hat{\mathbf{R}}_0^+(\mathbf{x}_R, \mathbf{x}_A, \omega)\hat{\mathbf{p}}^+(\mathbf{x}_A, \mathbf{x}_S, \omega) d^2\mathbf{x}, \tag{3}$$

where we substituted $\hat{S}\hat{\mathbf{R}}_0^+ = \hat{\mathbf{p}}_0^+$, with $\hat{\mathbf{R}}_0^+$ being the reflection response of the medium below the receiver array, which we can write as

$$\hat{\mathbf{R}}_0^+ = \begin{pmatrix} \hat{R}_{0,PP}^+ & \hat{R}_{0,PSv}^+ & \hat{R}_{0,PSh}^+ \\ \hat{R}_{0,SvP}^+ & \hat{R}_{0,SvSv}^+ & \hat{R}_{0,SvSh}^+ \\ \hat{R}_{0,ShP}^+ & \hat{R}_{0,ShSv}^+ & \hat{R}_{0,ShSh}^+ \end{pmatrix}, \tag{4}$$

where $\hat{R}_{0,XY}^+$ represents the reflection response relating the reflected X-mode to the incident Y-mode. The purpose of MDD is to solve this integral in a least-squares sense. This method is closely related to Betti Deconvolution (Amundsen, 1999; Holvik and Amundsen, 2005) and Least-Squares Redatuming (Schuster and Zhou, 2006). First we discretize equation 3 as

$$\hat{\mathsf{P}}^- = \hat{\mathsf{R}}_0^+ \hat{\mathsf{P}}^+. \tag{5}$$

Here $\hat{\mathsf{P}}^{\pm}$ is a matrix of vectors $\hat{\mathbf{p}}^{\pm}(\mathbf{x}_R, \mathbf{x}_S, \omega)$, where the columns have fixed source type and location but variable receiver type and location and the rows have fixed receiver type and location but variable source type and location. $\hat{\mathsf{R}}_0^+$ is a matrix of multi-component reflection matrices $\hat{\mathbf{R}}_0^+(\mathbf{x}_R, \mathbf{x}_A, \omega)$. Equation 2 can be solved by least-squares inversion as

$$\hat{\mathsf{R}}_0^+ \approx \hat{\mathsf{P}}^- \left\{\hat{\mathsf{P}}^+\right\}^\dagger \left[\hat{\mathsf{P}}^+ \left\{\hat{\mathsf{P}}^+\right\}^\dagger + \varepsilon^2 \mathsf{I}\right]^{-1}, \tag{6}$$

where ε is introduced as a stabilization factor, superscript $\dagger$ denotes the complex-conjugate transpose and I is the identity matrix. If we approximate the term between square brackets by the identity matrix, we are left with

$$\hat{\mathsf{R}}_0^+ \approx \hat{\mathsf{P}}^- \left\{\hat{\mathsf{P}}^+\right\}^\dagger, \tag{7}$$

which can be written in integral notation as

$$\hat{\mathbf{R}}_0^+(\mathbf{x}_R, \mathbf{x}_A, \omega) = \int_{\partial Ds} \hat{\mathbf{p}}^-(\mathbf{x}_R, \mathbf{x}_S, \omega)\left\{\hat{\mathbf{p}}^+(\mathbf{x}_A, \mathbf{x}_S, \omega)\right\}^\dagger d^2\mathbf{x}_S, \tag{8}$$

where the integral is over source locations $\mathbf{x}_S$. Equation 8 can be recognized as a multi-dimensional variant of the Virtual Source method for up- and downgoing wavefields, as suggested by Mehta et al. (2007). In the following example we will use both Multi-Dimensional Deconvolution and Cross-Correlation to demonstrate that the first can yield improvements in some particular cases.

Elastic Interferometry by Multi-Dimensional Deconvolution

Example

The P-wave velocity model and geometry for this example is shown in Figure 1. 1001 2-component sources are located at the surface, whereas the tractions and particle velocities are assumed to be known at the receiver level at 800m depth. We use visco-elastic finite difference modeling (Robertsson et al, 1994) to generate synthetic data with intrinsic losses, where we choose a Q-factor for P-waves $Q_P = 21$ and a Q-factor for S-waves $Q_S = 16$ at 30 Hz frequency. The wave fields are decomposed with equation 1 and redatumed to the receiver level by MDD (equation 8). We also generate a reference data set. This is done by replacing the medium above the receiver array with a homogeneous halfspace with similar properties as at the receiver array and placing multi-component sources at the receiver locations. The reference responses are decomposed with equation 1 at both the source and receiver side to generate the reference reflection matrix for $\hat{\mathbf{R}}_0^+(\mathbf{x}_R, \mathbf{x}_A, \omega)$. In Figure 2 we show 9 retrieved traces in red versus the reference data in black for the PP reflection response. Note that MDD was very successful in retrieving the correct response for this shot record. Next we compare the response with that of CC-based redatuming through equation 7 – see Figure 3. Note that the phase is still handled correct, but the amplitude to offset behavior is less accurate. This is even better visible if we present the amplitude spectra in the frequency-space domain. Figure 4 presents the amplitude spectrum of the PP reference response in the frequency-space domain. In Figure 5 we show the equivalent retrieved spectrum by CC-based interferometry. Note that the match with the reference response (Figure 4) is quite poor, due to the fact that the underlaying assumptions of CC-based interferometry are not exactly met. Proper handling of the inverse in equation 6, however, like we do in implementation of MDD, retrieves the amplitude spectrum more accurately, as we demonstrate in Figure 6. Next we redo the modeling without loss-terms but with corruption of uncorrelated noise within the seismic frequency bandwidth with amplitudes up to 30% of the maximum amplitude in the initial shot gathers. In Figure 7 we show an example of a noise corrupted shot record that was used as input. Once more we used equation 7 to apply MDD to redatum the field. As an example we show the PS-converted response in Figure 8. Note that also for these noise corrupted gathers, MDD is able to give a very reasonable prediction of both amplitude and phase.

Conclusion

We have tested elastic interferometry by Multi-Dimensional Deconvolution for its ability to handle intrinsic losses and noise. It is shown that MDD provides a very accurate response in dissipative media with better amplitude to offset characteristics than Cross-Correlation (CC) based methodology. Further MDD proofed stable under the corruption of random noise within the seismic frequency band.

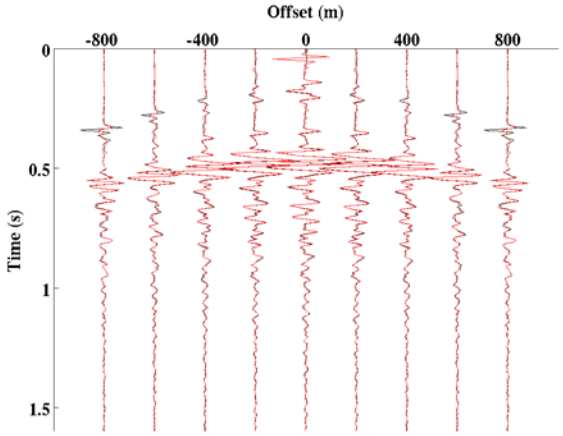

Figure 2: PP reflection response at the receiver level as retrieved by Multi-Dimensional Deconvolution (red), compared with a reference response (black) for a selection of 9 traces.

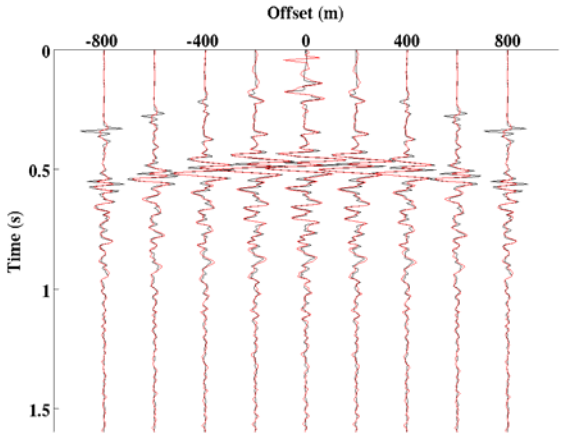

Figure 3: PP reflection response at the receiver level as retrieved by Cross-Correlation (red), compared with a reference response (black) for a selection of 9 traces.

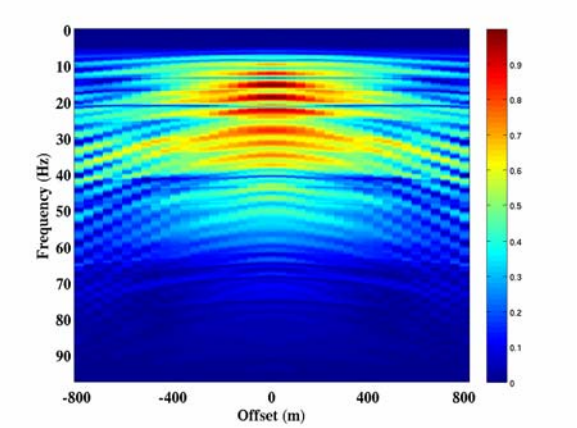

Figure 4: Amplitude spectrum of the reference PP response in the frequency-space domain.

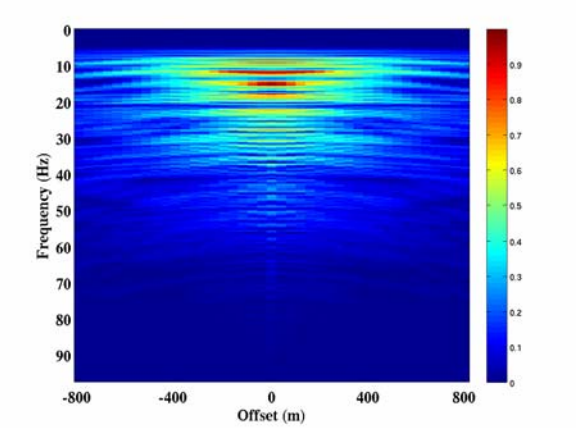

Figure 5: Amplitude spectrum of the PP reflection response in the frequency-space domain as retrieved by Cross-Correlation.

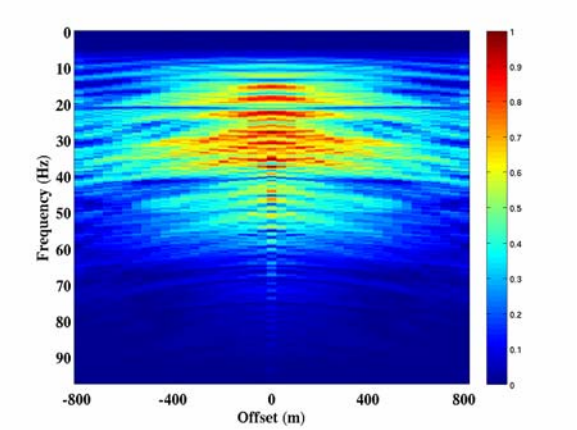

Figure 6: Amplitude spectrum of the PP reflection response in the frequency-space domain as retrieved by Multi-Dimensional Deconvolution..

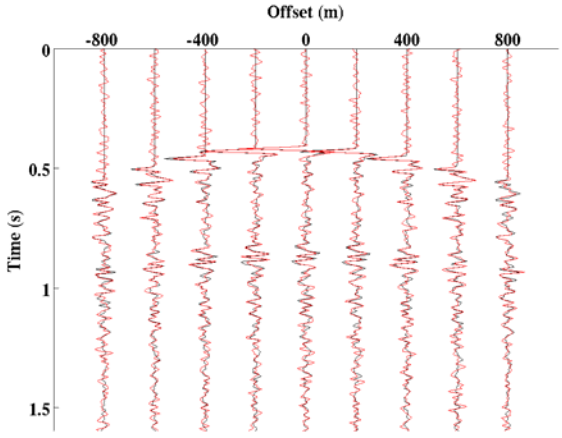

Figure 7: Example of a shot record corrupted wit uncorrelated noise (red) overlaying the same shot record without noise (black); a vertical force source was located at the earth surface and we show vertical particle velocities at 800m depth.

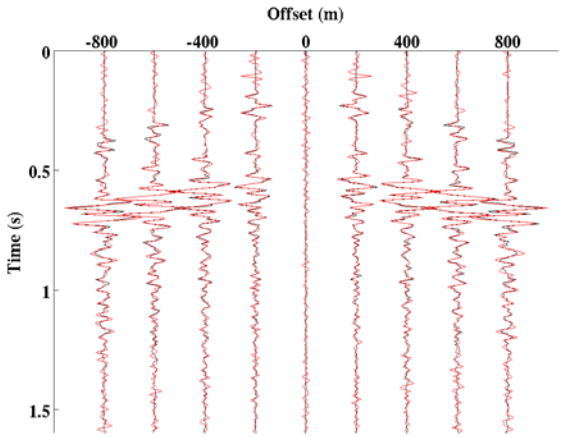

Figure 8: PS reflection response at the receiver level as retrieved by Multi-Dimensional Deconvolution (red), compared with a reference response (black) for a selection of 9 traces. Uncorrelated noise was added to the input data.

Acknowledgements

This work is supported by the Dutch Technology Foundation STW, applied science division of NWO and the Technology Program of the Ministry of Economic Affairs (grant DCB.7913).